Chemistry Europe
European Chemical Societies Publishing

WILEY VCH

Excellence in Chemistry Research

Announcing our new flagship journal

- Gold Open Access
- Publishing charges waived
- Preprints welcome
- Edited by active scientists

Meet the Editors of *ChemistryEurope*

Luisa De Cola
Università degli Studi di Milano Statale, Italy

Ive Hermans
University of Wisconsin-Madison, USA

Ken Tanaka
Tokyo Institute of Technology, Japan

ChemistrySelect

Research Article
doi.org/10.1002/slct.202204904

Chemistry Europe
European Chemical Societies Publishing

www.chemistryselect.org

P1 Push-Pull Dye as a Case Study in QM/MM Theoretical Characterization for Dye-sensitized Solar Cell Organic Chromophores**

Valeria D'Annibale,[a, b] Cheng Giuseppe Chen,[a] Matteo Bonomo,[a, c] Danilo Dini,[a] and Marco D'Abramo*[a]

In this work, an accurate modelling of the absorption spectrum and of the ground and excited state redox properties of the P1 dye – a benchmark system in p-type Dye-sensitized Solar Cells (p-DSCs) – is presented. The computed values were obtained by means of a QM/MM approach that combines a low computational cost with a proper treatment of the effects of the environment. The good agreement between our theoretical-computational estimates and the available experimental data underlines how a proper description of the redox thermodynamics of the ground and electronic excited states of the dye in a realistic environment can be provided by *in silico* modelling.

Introduction

Dye-sensitized solar cells (DSCs) are photoelectrochemical devices that convert solar energy into electrical energy,[1,2] thanks to the photoactivated injection of charge carriers from a large band gap semiconductor to a redox species, via an electronically excited molecular dye.[3,4]

At the practical level, DSCs attract continuous attention in the ambit of organic/molecular photovoltaics by virtue of the optical (quasi-)transparency, a feature that allows the integration of DSCs in building fenestration and the development of powering systems based on the exploitation of indoor-light.[5] From a computational viewpoint, Quantum Mechanics/Molecular Mechanics (QM/MM) approaches, able to couple the electronic description of a region of the system with an extended phase-space sampling, have been applied in the past to model the one-electron oxidation occurring in complex environments such as in biological systems[6–9] and in organic molecules in solution.[10–14] In the context of Dye-sensitized Solar Cells, it is worth noting that reduction/oxidation potentials are often simply modelled by considering the HOMO and LUMO energies, thus neglecting a proper physical description of such a property, which requires the estimation of the free energy of the redox processes.

In this work, we have selected, as case study, the P1 molecule (4-(Bis-4-[5-(2,2-dicyano-vinyl)-thiophene-2-yl]-phenyl-amino)-benzoic acid[15]), one of the first organic dye effectively used in p-type cells, originally designed, synthesized and characterized by Qin et al. as p-type benchmark dye and it was studied by means of a QM/MM procedure – the Perturbed Matrix Method (PMM)[16,17] – to describe the electronic properties of the dye in solution, where the environmental effects are explicitly treated.

By such an approach, it was possible to evaluate the redox properties, *i.e.* the free energies of the electron loss/gain processes, of the P1 molecule in a realistic environment, at a reduced computational cost and with a higher accuracy than DFT *ab initio* methods,[5,18–20] due to the perturbation given by Molecular Dynamics (MD) sampling. The presence of the environment, classically treated, enables a realistic description, without the limit in computational cost that other QM/MM methods generally reveal.[21] In particular, we estimated the reduction and the oxidation potential of the ground and the first electronic excited state of the P1 molecule as well as its absorption spectrum in solution.

From a practical point of view, in a real DSC environment, the light absorbing dye needs to be chemically linked to the semiconductor via a covalently-bound anchoring group present in the dye structure, in order to impart chemical stability in the dye-sensitized system, during operations under illumination, and to warrant the continuity of the action of sensitization.[22] Anchoring allows the charge transfer (CT) between dye and the semiconductor electrode via effective decoupling of the photogenerated exciton.[23]

At the photoactive dye-semiconductor junction of a DSC, the electron transfer (*et*) process between the excited dye and a redox species is rendered possible for the matching of the frontier energy levels of the dye and the Nernst energy level of

[a] *Dr. V. D'Annibale, Dr. C. G. Chen, Dr. M. Bonomo, Prof. D. Dini, Prof. M. D'Abramo*
Department of Chemistry, Sapienza University of Rome, 00185 Rome, Italy
E-mail: marco.dabramo@uniroma1.it
[b] *Dr. V. D'Annibale*
Department of Basic and Applied Sciences for Engineering, Sapienza University of Rome, 00185 Rome, Italy
[c] *Dr. M. Bonomo*
Department of Chemistry and NIS Interdepartmental Center, University of Turin, Turin, Italy

[**] *QM/MM: Quantum Mechanics/Molecular Mechanics*

Supporting information for this article is available on the WWW under https://doi.org/10.1002/slct.202204904

the redox couple,[24] according to the scheme depicted in Figure 1, for a p-type DSC.[25,26]

Organic chromophores for p-type cells are capable to push the photo-generated electron excess away from the site of anchoring on p-type electrode substrate (conducting by holes), through a structural spacer which is vehicular for electrons[27,28] (Figure 2).

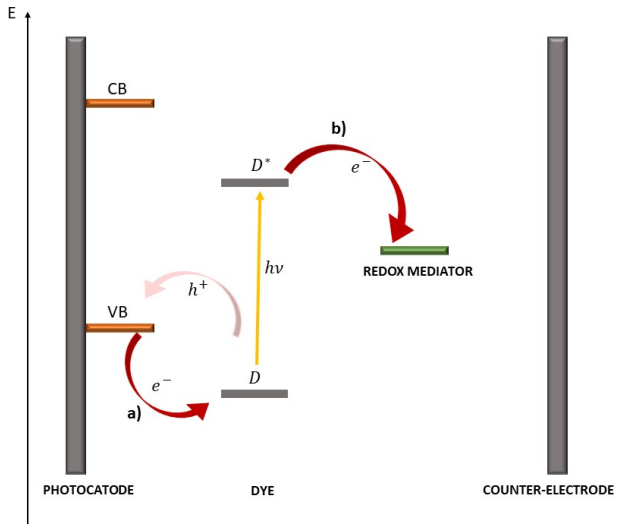

Figure 1. Electron pathway (indicated by the red arrows) in an illuminated p-type DSC for the realization of two *et* steps: (*a*) p-type semiconductor→dye (*et* between the states with energies corresponding respectively to the upper edge of the p-type semiconductor valence band (VB) and the ground state of the dye); (*b*) excited dye→oxidized form of the redox couple (*et* between the excited dye energy level and the empty state of the oxidized form of the redox mediator). Upon light absorption (consisting in the excitation of the anchored dye), the overall process of *et* between p-type semiconductor and redox species occurs through the succession of steps (*a*) and (*b*).

Therefore, an important part of the p-DSC research is represented by the design and modelling of new dye-sensitizers to ameliorate the conversion performance of such photoelectrochemical devices.[29,30]

This kind of dye structures belongs to the wider class of push-pull dyes,[15,31–36] which have an electron-donor moiety separated by one or more spacer units – usually aromatic rings – and an additional sub-unit with electron-withdrawing character. This structural arrangement of chemical moieties, with different electronic properties, favors an intramolecular CT process[37] and defines an *et* pathway from the semiconductor to the redox mediator in solution.

Generally, the efficiency of p-type cells is remarkably lower than that of n-type[38–40] and it is related to the possibility of charge recombination (between holes in the semiconductor and the reduced dye or the reduced form of the redox mediator)[41–43] and/or of dye aggregation (with an intermolecular charge transfer, thus decreasing the effectiveness of the electron injection between the semiconductor and the dye molecules).

For this reason, the *in silico* analysis of the electronic features of new organic chromophores might provide a boost in designing more efficient Dye-sensitized Solar Cells. In fact, computational modelling of the electronic structure of typical organic dyes, used in these devices, embedded in a solvent box, can be accomplished by a relatively low amount of resources in terms of time and computational power. Following well-established theoretical-computational approaches, routinely and effectively used in different fields, an accurate modelling of the dye might provide a better understanding of the electronic processes regulating the DSCs behaviour, thus suggesting alternative and effective strategies for the improvement of such devices.

In P1 dye molecule,[15] the electron-donor moiety is represented by a triphenylamine unit, whereas the electron-

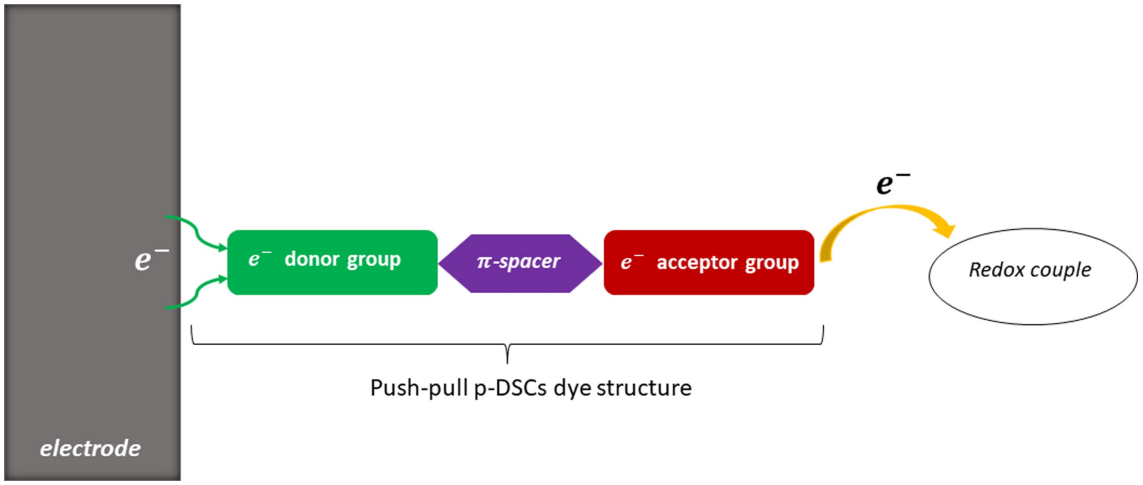

Figure 2. Structure of a dye for p-DSCs, characterized by the presence of three distinct parts, each of one with a specific function: (*green*) electron donor (region of the dye that receives an electron from a p-type semiconducting substrate and is able to donate it to an electron acceptor moiety of the molecule); (*violet*) π-bridge (electron vehicle); (*red*) electron acceptor (region of the dye that withdraws the electron from the donor counterpart and is able to donate it to the oxidized form of the redox mediator). All moieties are electrically connected with each other. The desired *et* process is activated by light-absorption (an event that leads to charge separation in the π-bridge moiety).

withdrawing moiety is constituted by two malononitrile units. Tiophene rings are used as spacers, with the role of reducing the planarity of the structure to avoid aggregation between dye molecules and to slow down charge recombination phenomena. Here, the electrons flow from the donor part of the molecule to the malononitrile acceptor groups located on the opposite side of the structure, resulting in an electron deficiency near the p-type semiconductor surface. The *et* pathway ends as the excess electron, localized on the malononitrile moieties, is transferred to the redox species in the electrolyte. According to these considerations, our data, in close agreement with experimental values, suggest that this kind of approach can be used to model dye-systems, taking into account the electronic properties of the molecules with great accuracy and evaluating their spectroscopic and redox features, thus allowing for an *in silico* screening of the most promising molecules.

Results and Discussion

Energetic of the P1 molecule in solution

The unperturbed (gas-phase) properties, *i.e.* excitation energies (reported in Table S3–S5 of SI), ESP charges and dipole moments, have been calculated and used – within the PMM procedure – to estimate the perturbed properties, as explained in the Methods section (see Theoretical background, Eq. (1–3)). Due to its rigid structure, the QC is represented by the whole P1 molecule. Such a choice is supported by the analysis of the dihedral angles (reported in Panel S3 of SI), which shows that limited intervals of dihedral angle values are explored along the MD trajectories. The analysis of the change in the charge distribution upon excitation indicates how the charge is able to flow through the dye, in virtue of its typical push-pull structure, upon excitation by solar radiation. In particular, the difference between the unperturbed charge density of the ground and the first excited state shows a positive charge density difference in the electron-donor portion and a negative charge density difference in the two electron-acceptor moieties of the dye. The corresponding map of the charge density differences and the associated atomic charges are reported in Figure 3 and Table 1.

By means of the PMM, we estimated the effects of the environment on the electronic energy of the P1 molecule in both cationic and anionic forms. As expected, the effect of the environment is to lower the electronic energy of the dye for all the forms considered (see Table 2). Such an effect is particularly relevant in the ionic ensembles, where the energy decreases are – on average – of 3.60 eV (Radical Anion ensemble, RA) and 4.77 eV (Radical Cation ensemble, RC), due to the favourable electrostatic interactions taking place between the chromophore and the solvent molecules.

However, the energy decrease of the neutral molecule due to the environment is more limited with respect to the ionic forms, indicating that the energies of the reduction and oxidation processes are both affected by the environment.

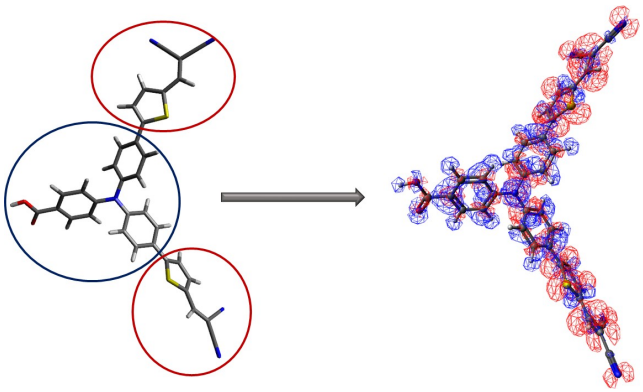

Figure 3. *Left*: Stick representations of the P1 molecules. The electron-withdrawing regions are indicated by red circles, while the electron-donor one, by a blue circle. C atoms are in gray, N atoms in blue, O atoms in red, S atoms in yellow and H in white. *Right*: Density charge differences between the first excited state and the ground state. Red/blue surfaces indicate an increase/decrease of the electronic density upon electronic excitation.

Table 1. P1 neutral form ESP charges of the electron-donor (TRPH) and electron-withdrawing (S1) moieties. Δq is the difference between the first excited state and the ground state ESP atomic charges.

Charge Density (a.u.)	TRPH	S1
ground state	0.24	−0.24
1st excited state	0.61	−0.61
Δq	0.37	−0.37

Table 2. Effects of the environment on the electronic energies for the neutral ($\langle \mathcal{U}_e \rangle_N - \mathcal{U}^0_{e,N}$), radical anion ($\langle \mathcal{U}_e \rangle_{RA} - \mathcal{U}^0_{e,RA}$) and radical cation ($\langle \mathcal{U}_e \rangle_{RC} - \mathcal{U}^0_{e,RC}$) states of the dye molecule. $\mathcal{U}^0_e$ represents the unperturbed electronic ground state energy. The energies are in eV.

Molecule	$\langle \mathcal{U}_e \rangle_N - \mathcal{U}^0_{e,N}$	$\langle \mathcal{U}_e \rangle_{RA} - \mathcal{U}^0_{e,RA}$	$\langle \mathcal{U}_e \rangle_{RC} - \mathcal{U}^0_{e,RC}$
Neutral Ensemble	−1.38	−1.28	−1.61
Radical Anion Ensemble	−1.47	−3.60	
Radical Cation Ensemble	−2.14		−4.77

Furthermore, Figure 4 shows the unperturbed state contribution to the perturbed ones. The stabilization of the radical anion/cation molecules, in their respective ionic ensemble, is due to favourable electrostatic interactions which induce a mixing of the unperturbed states, whose effect is to lower the perturbed energy in comparison with the neutral ensemble. On the other hand, P1 dye in the neutral form presents a very limited mixing between the unperturbed states in all of its perturbed states (for a detailed analysis of the ground perturbed electronic wavefunctions in the three environments considered, see Figure S3 of SI).

By means of MD-PMM approach, we also estimate the vertical ionization energy (VIE) as explained in Methods section. To check the effect of the conjugation on this property, the VIE was calculated using different QC of different sizes. Interestingly, the effect of adding conjugated groups to the thiophene-malonitrile is to lower the VIE, which reaches the

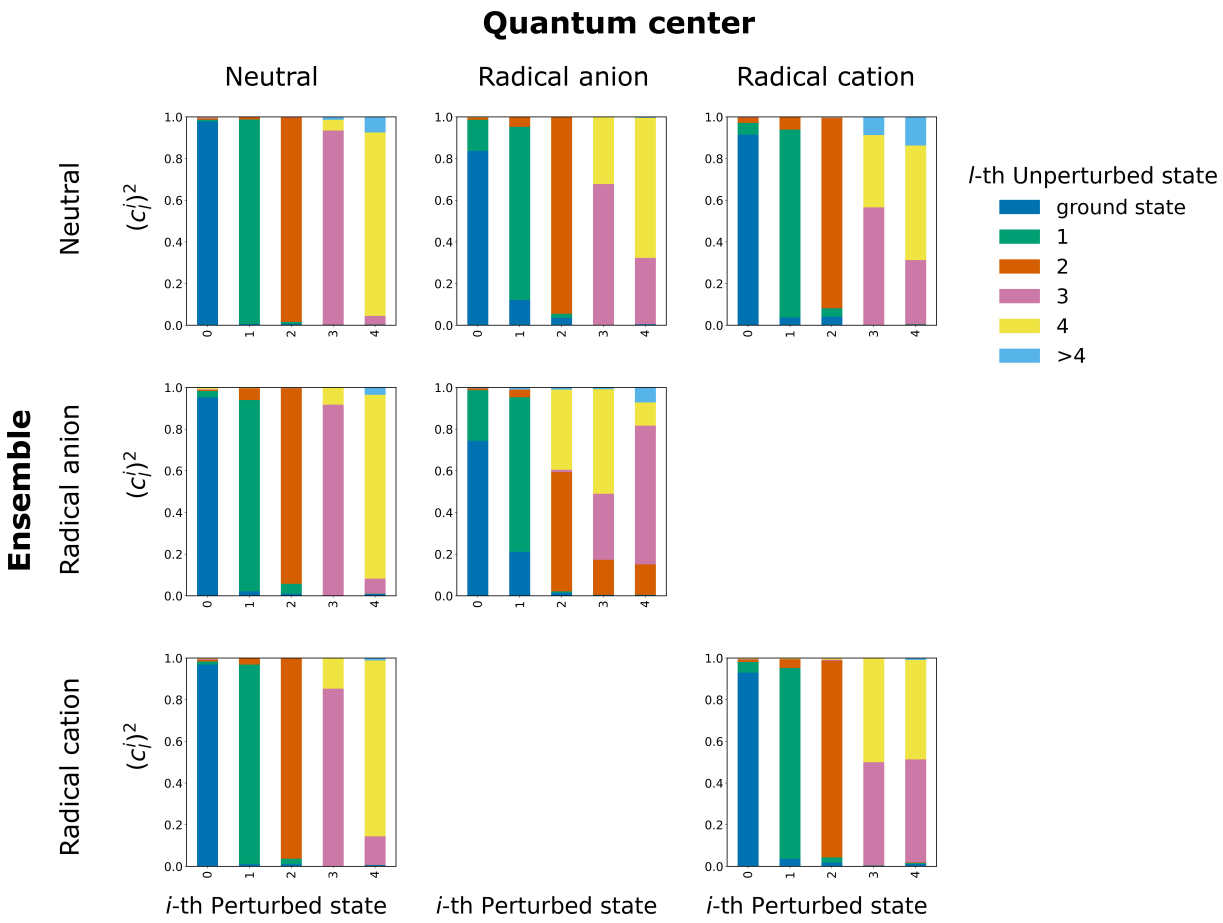

Figure 4. Cumulative histograms of the contributions of the unperturbed electronic states to the perturbed electronic states, for each QC (neutral, radical anion and radical cation) in the three ensembles (neutral, radical anion and radical cation). The contributions were averaged over the entire simulations.

value of 6.91 eV when the whole P1 molecule is taken as QC (see Table S6 in SI). As expected, and in contrast to the redox free energy (see below), the convergence of the VIEs requires a rather limited sampling, *i.e.* it converges in the first few ns of the simulation (see Panel S1 in SI). Using the trajectory of the perturbed energy differences, the reduction/oxidation free energies, as well as the corresponding redox potentials have been calculated by means of Eq. (5–6) and Eq. (4), respectively (see below). Our theoretical-computational estimates of the redox potentials, reported in Table 3, are in very good agreement with the corresponding experimental data. In fact, within the statistical uncertainty evaluated by block averaging procedure of ≈0.1 V, both the calculated reduction and oxidation potentials of P1 in acetonitrile solution are virtually indistinguishable from the experimental values (Table 3). Interestingly, the estimate of the free energies indicates that, for the dye in solution, a proper phase space sampling of the whole system is mandatory. In fact, the redox free energy values calculated along the MD trajectories (Panel S2 in SI) clearly show that the convergence of this property is achieved only after several ns.

Table 3. Comparison between the experimental reduction and oxidation potential[15,44,45] and the values calculated by means of PMM in acetonitrile solution, with an estimated error of ±0.1 V. All the redox potentials are reported against V_{NHE} = 4.43 V.

	V_{red}	V_{ox}
ACN sol.		
exp.[a]	−0.81	1.34
calc. (PMM)	−0.75	1.22

[a] Experimental values are reported as the mean potential between three different data present in literature,[15,44,45] with an estimated error of ±0.03 V for both reduction and oxidation processes.

As in DSCs the electronic excited state potentials can be involved in the process, we also calculated, using the same procedure, the redox potentials of the first excited state of the dye, obtaining a $V_{red,\ exc}$ of −1.38 V and a $V_{ox,\ exc}$ of 1.93 V (see Table 4). Our data underline that the first excited state of P1 shows a lower stabilization of the anionic form in the excited state with respect to the ground state as provided by the corresponding free energy differences (see Table 4). Similarly, the oxidation of the ground state is favoured with respect to the excited state.

In summary, the calculated oxidation potentials of the P1 molecule in solution, for both the ground and the first excited

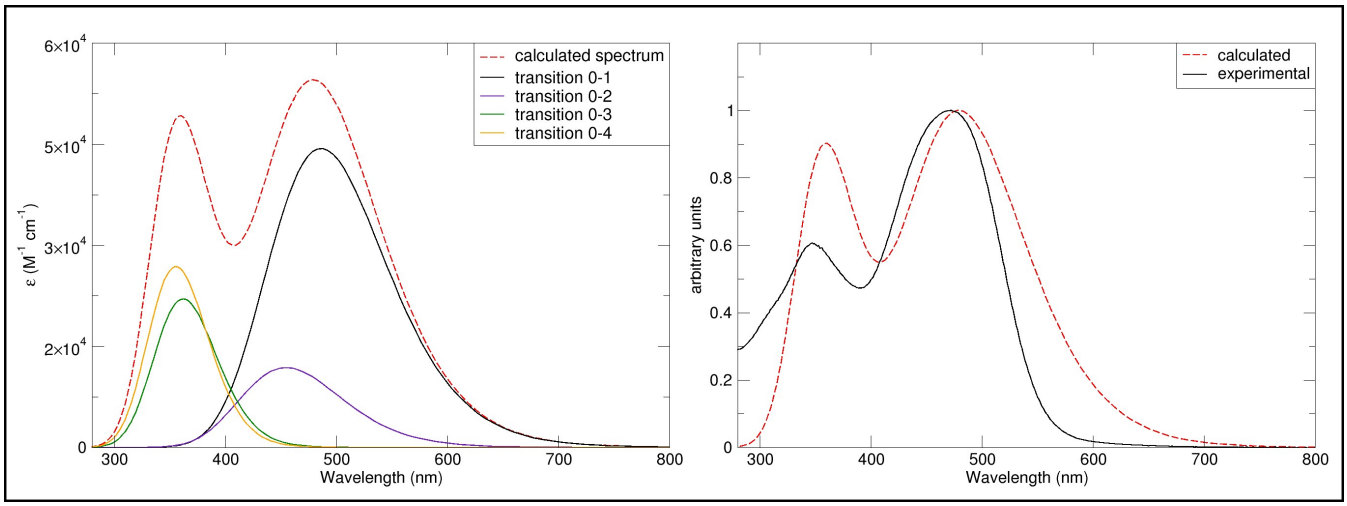

Figure 5. *Left*: Theoretical absorption spectrum with the contributions of the first four excited states. *Right*: Comparison between normalized theoretical and experimental P1 absorption spectra.

electronic states, are more positive than the NiO valence band (≈0.5 V vs NHE[45,46]), thus allowing for a hole injection to the NiO from both the electronic states. Similarly, the P1 reduction potential in solution decreases of ≈0.6 V upon light absorption, thus indicating that, in both the electronic states, the redox reaction involving the reduction of the usual redox mediator, *i.e.* the couple I_3^-/I^-, and the P1 (or P1*) oxidation is thermodynamically favoured.

Uv-Vis Absorption

The simulated Uv-Vis absorption spectrum was calculated as reported in Eq. (7–8) and compared with the experimental one in the range between 280 and 800 nm (see Figure 5). Both the calculated λ_{max} and $\varepsilon(\lambda_{max})$ well match the corresponding experimental data (see Table 5).

The analysis of the excited electronic states shows that the first two electronic transitions are responsible for the first band centered at ≈480 nm, whereas the third and fourth excited states contribute to the band centered around 370 nm. The differences between the calculated and the measured spectra in this region are probably due to additional excited states which are not well described by gas-phase quantum mechanical calculations.

The effect of the perturbation on the excitation energies can be evaluated by the comparison between the gas-phase values and the corresponding perturbed excitation energies. As shown in Table 6, the energy shift between unperturbed and perturbed excitation energies is always positive, indicating a more favourable interaction of the environment with the ground state with respect to the excited states.

In addition to this, the effect of considering the environment perturbation (*i.e.* acetonitrile solvent), is highlighted also by the different Uv-Vis spectrum between *in vacuum* and MD-PMM calculations, as reported in Figure S2 and Table S2 of SI. The perturbation enables a more accurate modelling of both the λ maximum position and the relative height of the two main absorption peaks.

Table 4. Free energy differences and redox potentials for the oxidation and reduction processes of the dye in the ground and in the 1st excited state. The estimated statistical error for the energies is ∼ ±0.1 eV and for the redox potentials (reported Vs V_{NHE} = 4.43 V) is ∼ ±0.1 V.

Ground state	ΔA (eV)	$V^{PMM}_{red/ox}$ (V)
$D + e^- \rightleftharpoons D^{-\bullet}$	−3.7	−0.75
$D \rightleftharpoons D^{+\bullet} + e^-$	5.7	1.22
1st excited state		
$D^* + e^- \rightleftharpoons [D^{-\bullet}]^*$	−3.0	−1.38
$D^* \rightleftharpoons [D^{+\bullet}]^* + e^-$	6.4	1.93

Table 5. Comparison between perturbed (E^{pert}_{exc}) and unperturbed (E^{unpert}_{exc}) excitation energies. Values are reported in eV.

Transition	E^{pert}_{exc}	E^{unpert}_{exc}
0→1	2.54	2.45
0→2	2.74	2.65
0→3	3.43	3.34
0→4	3.49	3.41

Table 6. Experimental and Theoretical spectral parameters.

	λ_{max} (nm)	ε (λ_{max}) ($M^{-1}\,cm^{-1}$)
Theoretical	479	54544
Experimental	472	58569

Conclusion

In our work we show the possibility of accurately reproducing the electronic properties of a dye, the P1 molecule, by means of a theoretical-computational procedure at a reasonable computational cost. Noteworthy, the P1 reduction/oxidation potentials in solution are formally estimated by the free energy differences, thus not requiring further assumptions on orbital energy levels.

The calculated redox properties and the Uv-Vis absorption spectrum are in very good agreement with the corresponding experimental data in acetonitrile solution. In addition, our procedure is able to model the redox properties of the dye electronic excited states, which can be involved in the DSCs. In particular, our data point out that the change in redox potentials upon light absorption still allows for the redox processes occurring within DSCs, *i.e.* the hole injection in the semiconductor and the dye oxidation by the redox mediator. Therefore, the proposed method represents a valid tool to test and design molecules with selected electronic features to be used in Dye-sensitized Solar Cells.

Methods

Theoretical background

The Perturbed Matrix Method

The MD-PMM is a theoretical approach similar to other Quantum Mechanics/Molecular Mechanics (QM/MM) hybrid methods.[14,47–51] In such approaches, molecular dynamics simulations usually provide a proper sampling of the molecule configurations and a sub-part of the overall system is considered as quantum center (QC), *i.e.* where the electronic properties are explicitly calculated by means of quantum-mechanical calculations.[7] The QC is the region of the system where the electronic processes are observed. The details of the method can be found in previous works[7,16,17] and thus, only a brief description is reported here.

The electronic unperturbed properties of the isolated QC are calculated at quantum-mechanical level in vacuum. Then, for each step of the molecular dynamics simulation, the instantaneous configuration of the environment atoms determines different charge distributions providing the perturbing electric field felt by the QC. This effect is included within the QC electronic Hamiltonian operator, $\hat{H}$, that can be expressed via:

$$\hat{H} = \hat{H}^0 + \hat{V} \tag{1}$$

where $\hat{H}^0$ is the unperturbed electronic Hamiltonian for the isolated QC and $\hat{V}$ is the perturbation operator, that can be obtained *via* a multipolar expansion centered in the QC center of mass, $\mathbf{r}_0$:

$$\hat{V} \cong \sum_j [\mathcal{V}(\mathbf{r}_0) - \mathbf{E}(\mathbf{r}_0) \cdot (\mathbf{r}_j - \mathbf{r}_0) + \ldots] q_j \tag{2}$$

with j running over all the QC particles (*i.e.*, nuclei and electrons), q_j the charge of the jth particle, $\mathbf{r}_j$ the corresponding coordinates, $\mathcal{V}$ the electrostatic potential exerted by the perturbing environment, and $\mathbf{E}$ the perturbing electric field ($\mathbf{E} = -\partial\mathcal{V}/\partial\mathbf{r}$). In the present work, a recent development of the PMM approach including higher order terms by expanding the perturbation operator around each atom of the QC (atom-based expansion)[17] is used. Within such an approach, the perturbation operator $\hat{V}$ is expanded within each Nth atomic region around the corresponding atomic center $\mathbf{R}_N$ (*i.e.*, the nucleus position of the Nth atom of the QC), providing:

$$\hat{V} \cong \sum_N \sum_j \Omega_N(\mathbf{r}_j) [\mathcal{V}(\mathbf{R}_N) - \mathbf{E}(\mathbf{R}_N) \cdot (\mathbf{r}_j - \mathbf{R}_N) + \ldots] q_j \tag{3}$$

with j running over all QC nuclei and electrons, N running over all QC atoms, and Ω_N a step function being null outside and unity inside the Nth atomic region. The expansion of the perturbing term is used in this work only for the Hamiltonian matrix diagonal elements, whereas the other Hamiltonian matrix elements are obtained by using the QC-based perturbation operator expansion within the dipolar approximation (Eq. (2)). For each frame of the molecular dynamics trajectory, the Hamiltonian matrix is constructed and diagonalized taking into account the instantaneous perturbation of the environment. As a result, it provides a continuous trajectory of perturbed eigenvalues and eigenvectors, used here to estimate:

(i) QC ground and excited state energies for the neutral, oxidized and reduced form of the molecule;
(ii) QC perturbed transition dipole moments to describe the absorption signals in order to reproduce the Uv-Vis spectrum of the dye.

The Free Energy of the redox processes

The determination of the redox potentials requires the evaluation of the Helmholtz free energy change, ΔA, between the neutral and the oxidized/reduced forms of the molecule. The redox potential can be expressed as follows:

$$V_{red/ox} = -\frac{\Delta A_{red/ox}}{nF} \tag{4}$$

where F is the Faraday constant and n the number of the moles of exchanged electrons. In this way, for each electron transfer process, a free energy change can be expressed as:

$$\begin{aligned} &\Delta A = -k_B T \ln\langle e^{\beta\Delta\mathcal{H}}\rangle_{ox} + \Delta A^{ion}_{red} = \\ &k_B T \ln\langle e^{-\beta\Delta\mathcal{H}}\rangle_{red} - \Delta A^{ion}_{ox} \cong \\ &-k_B T \ln\langle e^{\beta\Delta\mathcal{U}_e}\rangle_{ox} + \Delta A^{ion}_{red} = \\ &k_B T \ln\langle e^{-\beta\Delta\mathcal{U}_e}\rangle_{red} - \Delta A^{ion}_{ox} \end{aligned} \tag{5}$$

where $\Delta\mathcal{H}$ is the QC-environment whole energy change upon oxidation ($red \rightarrow ox$) or reduction ($ox \rightarrow red$) process, while $\Delta\mathcal{U}_e$ is the corresponding QC perturbed electronic ground state

energy change that is obtained, at each classical configuration, from the relaxation of the quantum nuclear degrees of freedom. In these terms, the energy change is an adiabatic energy, approximating the vibronic ground state energy change[52] (*i.e.* $\langle \Delta \mathcal{U}_e \rangle_{red}$ is the adiabatic ionization energy, AIE). The angle brackets subscripts *ox* and *red* indicate that both the energy change, as well as the averaging, are obtained either in the oxidized or reduced ensemble, each involving its own ionic condition, and the approximation $\Delta \mathcal{H} \cong \Delta \mathcal{U}_e$ is used, since the environment internal energy change associated with the QC reaction is disregarded (being exactly zero when considering typical MD force fields and assuming the environment electronic state independent of the QC oxidation state).

Finally, ΔA_{red}^{ion} is the relaxation free energy for the reduced species due to the $ox \rightarrow red$ ionic environment transition and ΔA_{ox}^{ion} is the relaxation free energy for the oxidized species due to the $red \rightarrow ox$ ionic environment transition. From Eq. (5) it follows that $-k_B T \ln \left\langle e^{\beta \Delta \mathcal{U}_e} \right\rangle_{ox}$ and $k_B T \ln \left\langle e^{-\beta \Delta \mathcal{U}_e} \right\rangle_{red}$ provide the upper and lower bounds of ΔA and hence, assuming $\Delta A_{red}^{ion} \approx \Delta A_{ox}^{ion}$, it can be written:

$$\Delta A \cong \frac{k_B T}{2} \ln \frac{\left\langle e^{-\beta \Delta \mathcal{U}_e} \right\rangle_{red}}{\left\langle e^{\beta \Delta \mathcal{U}_e} \right\rangle_{ox}} \tag{6}$$

This last equation provides for the reduction, as well as the oxidation process, the perturbed free energy change evaluated by considering the average of the electronic ground state energy obtained via the MD-PMM approach described in the previous subsection. From the free energy values the redox potentials were consequently estimated (as shown in Eq. (9)).

Modelling of the Uv-Vis Absorption Spectrum

By means of the PMM-MD approach is possible to calculate the electronic properties of the ground and electronic excited states of QC in a complex environment[53] and thus, to model the absorption spectrum of chromophores in solution. Briefly, the absorption spectrum can be described by the extinction coefficients $\varepsilon_{0,i}(\nu)$ for the electronic transitions $0 \rightarrow n$ where n represents the excited state index. The extinction coefficient, $\varepsilon_{0,n}(\nu)$ can be expressed as:

$$\varepsilon_{0,n}(\nu) = \frac{|\mu_{0,n}|_\nu^2 \rho(\nu) h\nu}{6c\varepsilon_0 \hbar^2} \tag{7}$$

where ε_0 is the vacuum dielectric constant, $|\mu_{0,n}|_\nu^2$ is the square of the electronic transition dipole, averaged between the frequencies ν and $\nu + d\nu$, h is the Planck constant, $\hbar = \frac{h}{2\pi}$ and $\rho(\nu)$ is the probability density of the vertical transition frequency of the QC in the perturbing environment.[53] Along the N frames provided by the MD simulation, with ideally $N \rightarrow \infty$, we can rewrite the extinction coefficient as follows:

$$\varepsilon_{0,n}(\nu) = \lim_{N \rightarrow \infty} \frac{1}{N} \sum_{i=1}^{N} \frac{|\mu_{ref,i}|_\nu^2 \rho_i(\nu) h\nu}{6c\varepsilon_0 \hbar^2} \tag{8}$$

where $\rho_i(\nu)$ is the probability density of the vertical transition at the ith MD frame and $|\mu_{ref,i}|_\nu^2$ is the square of the perturbed transition dipole intensity at the ith MD frame, obtained for the reference QC structure, embedded in that instantaneous environment configuration.

Computational details

The PyMM open source software package was employed to apply the QM/MM hybrid method.[54] The PMM procedure was used considering the whole P1 molecule as the QC, whereas the acetonitrile molecules furnished the perturbation of the environment. Due to the very limited flexibility of the P1 (as suggested by the dihedral angle analysis, see Results and Discussion section and Panel S3 of SI), a single structure of the QC was used. The optimized geometries of the neutral, radical cation and radical anion dye molecule and their corresponding electronic ground state properties were obtained by means of the Density Functional Theory (DFT), using the mPW1PW91 functional and 6-31 + G(d,p) as basis set. The functional was selected according to the current literature dealing with charge transfer processes.[55,56] The unperturbed energies, dipole moments and atomic ESP charges for the excited states were computed at the same level of theory by means of the Time-Dependent Density Functional Theory (TD-DFT).[57,58] All the quantum-mechanical calculations have been performed by means of the Gaussian software package.[59] Molecular Dynamics (MD) simulations of the dye molecule in acetonitrile solution were performed by means of Gromacs software package.[60,61] The MD simulations provide, for both the redox processes analyzed, two ensembles with a respective ionic environment, each with the proper number of counterions to neutralize the total charge of the MD simulation box. All the dynamics were performed in a cubic box of side 4.08 nm at 300 K for 180 ns, with a time step of 2 fs, at constant volume, using a previously reported model of the acetonitrile.[62] The velocity rescaling algorithm has been used to keep the temperature constant at 300 K.[63] For the simulations of the molecule in (radical) cationic and anionic forms, the atomic partial charges were estimated by the same procedure used for determining the parameters provided in the OPLS-AA force field.[64] The carboxylic group atoms were kept fixed during the MD simulations to mimic the anchoring of the dye to a solid support. Furthermore, the absence of the semiconductor in our simulations, necessary for easy and inexpensive calculations, was considered as an unremarkable approximation, without a loss of accuracy, due to the fact that the spectra of P1 dye, free in acetonitrile or adsorbed to NiO semiconductor, show little variations (as reported by Qin et al.[15] in their supporting material). In addition, the dye molecules, anchored to the semiconductor, conduct the electron transfer at the interface between the solid surface and the solvent-electrolyte environment. In this respect, the last one results as the main responsible in modulating charge recombination processes that afflict p-type DSCs, thus making the modelling of the solvent the necessary condition for evaluating the electronic properties of the organic dyes in this context. For the reduction and oxidation potential calculation, we consider as reference the V_{NHE} value of 4.43 V, defining the standard redox potentials as follows:

$$\begin{aligned} V_{red} &= \frac{-\Delta A_{red}}{nF} - V_{NHE} \\ V_{ox} &= \frac{-\Delta A_{ox}}{nF} + V_{NHE} \end{aligned} \tag{9}$$

where V_{red} and V_{ox} are reduction/oxidation potentials associated to the following reactions:

$$\begin{aligned} D + e^- &\rightleftharpoons D^{-\bullet} \\ D &\rightleftharpoons D^{+\bullet} + e^- \end{aligned} \tag{10}$$

where D is the dye in its neutral form, while $D^{-\bullet}$ and $D^{+\bullet}$ indicate the radical anionic and cationic molecule, respectively. Also in this case, the free molecule in acetonitrile was considered as a valid comparison with the ciclovoltammetry data by Qin et al.,[15] collected in the same operative conditions. The redox potentials for the first excited state have been evaluated using the same procedure.

Furthermore, we have defined the average Vertical Ionization Energy (VIE) as $\langle \Delta \mathcal{U}_e \rangle_{red}$, with *red* subscript indicating that the calculation was performed in the reduced ensemble.

The estimates of the statistical errors for the observables calculated in this work were performed by block averaging procedure. That is, the value of the observable of interest was calculated in five sub-parts of the MD trajectory and the standard deviation of the mean was taken as a measure of the statistical inaccuracy of the observable.

The CT process from the electron-donor to the electron-acceptor moiety of the dye was also investigated by calculating the (unperturbed) charge density difference between the ground and the first excited state by means of the NWChem program.[65]

Experimental details

The Uv-Vis absorption spectrum of P1 dye (4-(Bis-4-[5-(2,2-dicyano-vynil)-tiophene-2-yl]-phenyl-amino)-benzoic acid)[15] was recorded on a Uv-Vis Spectrofotometer, Shimadzu UV-1700 Pharma Spec, using a quartz cuvette with an optical path of 1 cm and acetonitrile as solvent. As P1 dye, a commercial sample from Dyenamo AB was used in an acetonitrile solution 0.021 (±0.001) mM.

Acknowledgements

This work was partially funded by Sapienza University of Rome (progetti di Ateneo 2018/2019). The authors thank NVidia and CINECA for the computational support. D.D. acknowledges financial support from the University of Rome "La Sapienza" (Project ATENEO 2019, Prot. No. RM11916B756961CA), and from MIUR (Project PRIN 2017 with title "Novel Multilayered and Micro-Machined Electrode Nano-Architectures for Electrocatalytic Applications" – Prot. No. 2017YH9MRK). M.B. acknowledges financial support from the University of Rome "La Sapienza" (Project Avvio alla Ricerca – 2017, Prot. No. AR11715C7F641B8C). Open Access funding provided by Università degli Studi di Roma La Sapienza within the CRUI-CARE Agreement.

Conflict of Interest

No conflict of interest to declare.

Data Availability Statement

The data that support the findings of this study are available from the corresponding author upon reasonable request.

[1] B. O'Regan, M. Grätzel, *Nature* **1991**, *353*, 737.
[2] A. Hagfeldt, G. Boschloo, L. Sun, L. Kloo, H. Pettersson, *Chem. Rev.* **2010**, *110*, 6595.
[3] H. Gerischer, M. Michel-Beyerle, F. Rebentrost, H. Tributsch, *Electrochim. Acta* **1968**, *13*, 1509.
[4] M. Matsumura, S. Matsudaira, H. Tsubomura, M. Takata, H. Yanagida, *Ind. Eng. Chem. Prod. Res. Dev.* **1980**, *19*, 415.
[5] A. B. Muñoz-Garcia, I. Benesperi, G. Boschloo, J. J. Concepcion, J. H. Delcamp, E. A. Gibson, G. J. Meyer, M. Pavone, H. Pettersson, A. Hagfeldt, M. Freitag, *Chem. Soc. Rev.* **2021**, *50*, 12450.
[6] L. Shen, X. Zeng, H. Hu, X. Hu, W. Yang, *J. Chem. Theory Comput.* **2018**, *14*, 4948.
[7] L. Zanetti-Polzi, C. A. Bortolotti, E. Daidone, M. Aschi, A. Amadei, S. Corni, *Org. Biomol. Chem.* **2015**, *13*, 11003.
[8] M. D'Abramo, M. Orozco, A. Amadei, *Chem. Commun.* **2011**, *47*, 2646.
[9] C. M. Sterling, R. Bjornsson, *J. Chem. Theory Comput.* **2019**, *15*, 52.
[10] N. A. Murugan, S. Chakrabarti, H. Agren, *J. Phys. Chem. B* **2011**, *115*, 4025.
[11] G. Del Frate, F. Bellina, G. Mancini, G. Marianetti, P. Minei, A. Pucci, V. Barone, *Phys. Chem. Chem. Phys.* **2016**, *18*, 9724.
[12] M. Oftadeh, L. Tavakolizadeh, *Int. Nano Lett.* **2013**, *3*.
[13] P. Diamantis, J. F. Gonthier, I. Tavernelli, U. Rothlisberger, *J. Phys. Chem. B* **2014**, *118*, 3950.
[14] R. Seidel, M. Faubel, B. Winter, J. Blumberger, *J. Am. Chem. Soc.* **2009**, *131*, 16127.
[15] P. Qin, H. Zhu, T. Edvinsson, G. Boschloo, A. Hagfeldt, L. Sun, *J. Am. Chem. Soc.* **2008**, *130*, 8570.
[16] M. Aschi, R. Spezia, A. Di Nola, A. Amadei, *Chem. Phys. Lett.* **2001**, *344*, 374.
[17] L. Zanetti-Polzi, S. Del Galdo, I. Daidone, M. D'Abramo, V. Barone, M. Aschi, A. Amadei, *Phys. Chem. Chem. Phys.* **2018**, *20*, 24369.
[18] N. Martsinovich, A. Troisi, *Energy Environ. Sci.* **2011**, *4*, 4473.
[19] K. S. Keremane, A. Planchat, Y. Pellegrin, D. Jacquemin, F. Odobel, A. V. Adhikari, *ChemSusChem* **2022**, *15*, e202200520.
[20] S. Bhattacharya, S. M. Pratik, *Comput. Theor. Chem.* **2021**, *1199*, 113219.
[21] F. Mouvet, J. Villard, V. Bolnykh, U. Rothlisberger, *Acc. Chem. Res.* **2022**, *55*, 221.
[22] E. Galoppini, *Coord. Chem. Rev.* **2004**, *248*, 1283.
[23] A. Hagfeldt, U. B. Cappel, G. Boschloo, L. Sun, L. Kloo, H. Pettersson, E. A. Gibson, *Dye-sensitized Photoelectrochemical Cells*, Elsevier Inc. **2012**.
[24] M. Bonomo, A. Di Carlo, D. Dini, *J. Electrochem. Soc.* **2018**, *165*, H889.
[25] J. He, H. Lindström, A. Hagfeldt, S.-E. Lindquist, *Sol. Energy Mater. Sol. Cells* **2000**, *62*, 265.
[26] G. Naponiello, I. Venditti, V. Zardetto, D. Saccone, A. Di Carlo, I. Fratoddi, C. Barolo, D. Dini, *Appl. Surf. Sci.* **2015**, *356*, 911.
[27] A. Nattestad, A. J. Mozer, M. K. R. Fisher, Y.-B. Cheng, A. Mishra, P. Bäuerle, U. Bach, *Nat. Mater* **2010**, *9*, 31.
[28] S. Peiris, R. J. K. U. Ranatunga, I. R. Perera, *p-Type Dye Sensitized Solar Cells: An Overview of Factors Limiting Efficiency*, pages 315–344, Springer Singapore, Singapore **2020**.
[29] M. Bonomo, D. Saccone, C. Magistris, A. Di Carlo, C. Barolo, D. Dini, *ChemElectroChem* **2017**, *4*, 2385.
[30] M. Bonomo, N. Barbero, F. Matteocci, A. Di Carlo, C. Barolo, D. Dini, *J. Phys. Chem. C* **2016**, *120*, 16340.
[31] N. Cai, Y. Wang, M. Xu, Y. Fan, R. Li, M. Zhang, P. Wang, *Adv. Funct. Mater.* **2012**, *23*, 1846.
[32] C. J. Wood, G. H. Summers, E. A. Gibson, *Chem. Commun.* **2012**, *51*, 3915.
[33] G. García, C. Adamo, I. Ciofini, *Phys. Chem. Chem. Phys.* **2013**, *15*, 20210.
[34] A. Yella, C.-L. Mai, S. M. Zakeeruddin, S.-N. Chang, C.-H. Hsieh, C.-Y. Yeh, M. Grätzel, *Angew. Chem. Int. Ed.* **2014**, *53*, 2973.
[35] T. Higashino, K. Kawamoto, K. Sugiura, Y. Fujimori, Y. Tsuji, K. Kurotobi, S. Ito, H. Imahori, *ACS Appl. Mater. Interfaces* **2016**, *8*, 15379.
[36] A. Carella, F. Borbone, R. Centore, *Front. Chem.* **2018**, *6:481*.
[37] A. Maufroy, L. Favereau, F. B. Anne, Y. Pellegrin, E. Blart, M. Hissler, D. Jacquemin, F. Odobel, *J. Mater. Chem. A* **2015**, *3*, 3908.

[38] K. Kakiage, Y. Aoyama, T. Yano, K. Oya, J. I. Fujisawa, M. Hanaya, *Chem. Commun.* **2015**, *51*, 15894.
[39] U. Sultan, F. Ahmadloo, G. Cha, B. Gökcan, S. Hejazi, J.-E. Yoo, N. T. Nguyen, M. Altomare, P. Schmuki, M. S. Killian, *ACS Appl. Energy Mater.* **2020**, *3*.
[40] M. Bonomo, E. J. Ekoi, A. G. Marrani, A. Y. Segura Zarate, D. P. Dowling, C. Barolo, D. Dini, *Sustain. Energy Fuels* **2021**, *5*, 4736.
[41] P. Qin, M. Linder, T. Brinck, G. Boschloo, A. Hagfeldt, L. Sun, *Adv. Mater.* **2009**, *21*, 2993.
[42] Z.-D. Sun, M. He, K. Chaitanya, X.-H. Ju, *Mater. Chem. Phys.* **2020**, *248*, 122943.
[43] A. Daoud, A. Cheknane, A. Meftah, J. Michel Nunzi, M. Shalabi, H. S. Hilal, *Sol. Energy* **2022**, *236*, 10.
[44] J. Cui, J. Lu, X. Xu, K. Cao, Z. Wang, G. Alemu, H. Yuang, Y. Shen, J. Xu, Y. Cheng, M. Wang, *J. Phys. Chem. C* **2014**, *118*, 16433.
[45] P. Qin, J. Wiberg, E. A. Gibson, M. Linder, L. Li, T. Brinck, A. Hagfeldt, B. Albinsson, L. Sun, *J. Phys. Chem. C* **2010**, *114*, 4738–4748.
[46] A. Nattestad, M. Ferguson, R. Kerr, Y. B. Cheng, U. Bach, *Nanotechnology* **2008**, *19*.
[47] J. Gao, D. Truhlar, *Annu. Rev. Phys. Chem.* **2002**, *53*, 467.
[48] T. Vreven, K. Morokuma, Chapter 3 Hybrid Methods: ONIOM(QM:MM) and QM/MM, volume 2 of *Annu. Rep. Comput. Chem.*, pages 35–51, Elsevier **2006**.
[49] H. Lin, D. Truhlar, *Theor. Chem. Acc.* **2007**, *117*, 185.
[50] H. M. Senn, W. Thiel, *Angew. Chem. Int. Ed.* **2009**, *48*, 1198.
[51] M. Liu, Y. Wang, Y. Chen, M. J. Field, J. Gao, *Isr. J. Chem.* **2014**, *54*, 1250.
[52] V. D'Annibale, A. N. Nardi, A. Amadei, M. D'Abramo, *J. Chem. Theory Comput.* **2021**, *17*, 13011307.
[53] M. D'Alessandro, M. Aschi, C. Mazzuca, A. Palleschi, A. Amadei, *J. Chem. Phys.* **2013**, *139*, 114102.
[54] C. G. Chen, A. N. Nardi, A. Amadei, M. D'Abramo, *J. Chem. Theory Comput.* **2023**, *19*, 33.
[55] C. Adamo, V. Barone, *J. Chem. Phys.* **1998**, *108*, 664.
[56] B. J. Lynch, D. G. Truhlar, *J. Phys. Chem. A* **2001**, *105*, 2936.
[57] E. Runge, E. K. U. Gross, *Phys. Rev. Lett.* **1984**, *52*, 99.
[58] D. Jacquemin, A. Planchat, C. Adamo, B. Mennucci, ,*J. Chem. Theory Comput.* **2012**, *8*, 2359.
[59] M. J. Frisch, G. W. Trucks, H. B. Schlegel, G. E. Scuseria, M. A. Robb, J. R. Cheeseman, G. Scalmani, V. Barone, G. A. Petersson, H. Nakatsuji, X. Li, M. Caricato, A. V. Marenich, J. Bloino, B. G. Janesko, R. Gomperts, B. Mennucci, H. P. Hratchian, J. V. Ortiz, A. F. Izmaylov, J. L. Sonnenberg, D. Williams-Young, F. Ding, F. Lipparini, F. Egidi, J. Goings, B. Peng, A. Petrone, T. Henderson, D. Ranasinghe, V. G. Zakrzewski, J. Gao, N. Rega, G. Zheng, W. Liang, M. Hada, M. Ehara, K. Toyota, R. Fukuda, J. Hasegawa, M. Ishida, T. Nakajima, Y. Honda, O. Kitao, H. Nakai, T. Vreven, K. Throssell, J. A. Montgomery, Jr., J. E. Peralta, F. Ogliaro, M. J. Bearpark, J. J. Heyd, E. N. Brothers, K. N. Kudin, V. N. Staroverov, T. A. Keith, R. Kobayashi, J. Normand, K. Raghavachari, A. P. Rendell, J. C. Burant, S. S. Iyengar, J. Tomasi, M. Cossi, J. M. Millam, M. Klene, C. Adamo, R. Cammi, J. W. Ochterski, R. L. Martin, K. Morokuma, O. Farkas, J. B. Foresman, D. J. Fox, Gaussian16 Revision C.01 **2016**, gaussian Inc. Wallingford CT.
[60] E. L. B. H. M. J. Abraham, D. van der Spoel, the GRO-MACS development team, *GROMACS User Manual version 2019* **2019**.
[61] M. J. Abraham, T. Murtola, R. Schulz, S. Páll, J. Smith, B. Hess, E. Lindahl, *SoftwareX* **2015**, *1–2*, 19.
[62] C. Caleman, P. J. Van Maaren, M. Hong, J. S. Hub, L. T. Costa, D. Van Der Spoel, *J. Chem. Theory Comput.* **2012**, *8*, 6.
[63] G. Bussi, D. Donadio, M. Parrinello, *J. Chem. Phys.* **2007**, *126*, 014101.
[64] M. L. Price, D. Ostrovsky, W. L. Jorgensen, *J. Comput. Chem.* **2001**, *22*, 1340.
[65] E. Aprà, et al., *J. Chem. Phys.* **2020**, *152*.

Submitted: December 19, 2022
Accepted: March 16, 2023